Impact of Hysteresis Losses in Hybrid (HTS-LTS) Coils for Fusion Applications

(Article begins on next page)

04 May 2024

RESEARCH ARTICLE

Impact of Hysteresis Losses in Hybrid (HTS-LTS) Coils for Fusion Applications

ANDREA ZAPPATORE[1], **GIANLUCA DE MARZI**[2], **AND DAVIDE UGLIETTI**[3]

[1]NEMO Group, Dipartimento Energia, Politecnico di Torino, 10129 Turin, Italy
[2]Superconductivity Section, FSN Department, ENEA, 00044 Frascati, Italy
[3]Swiss Plasma Center (SPC), École Polytechnique Fédérale de Lausanne (EPFL), Villigen, 5232 Lausanne, Switzerland

Corresponding author: Andrea Zappatore (andrea.zappatore@polito.it)

ABSTRACT Several conductor designs featuring High Temperature Superconducting (HTS) stacked tapes for fusion coils are being proposed. These conductors are planned to operate in time-varying magnetic field and current; thus, the estimation of AC losses is fundamental for the conductor design and the accurate analysis of its performance in operation. The case study of an HTS conductor proposed for the hybrid (HTS-LTS) Central Solenoid coil for the EU DEMO tokamak is considered in this work. Here, a numerical model based on the finite element method (FEM) and the H-formulation is used, in order to estimate the hysteresis losses. The FEM model is first benchmarked against available analytical formulae as well as available literature data. Then it is applied to the real case operational scenario. It is shown that for the conductor design analyzed, the coupling losses are orders of magnitude lower than the hysteresis ones. The impact of the hysteresis+coupling losses on the temperature margin of the coil is assessed with a thermal-hydraulic model. It is shown that the heat generated in the HTS layers is partially transferred to the LTS layers, leading these layers to quench. An alternative conductor concept is also analyzed, showing that, however, in the top and bottom modules of the CS coil, due to the bending of the magnetic field, a too large heat deposition is present.

INDEX TERMS Superconducting magnets, nuclear fusion reactors, numerical modeling, electro-magnetics, thermal-hydraulics.

I. INTRODUCTION

The quest for high current, high field conductors based on High Temperature Superconductors (HTS) and in particular Rare-earth Barium Copper Oxide (REBCO) coated conductor for nuclear fusion applications is ongoing [1]. Some projects are considering the possibility to include them in the design, such as in the EU DEMO design [2] of the Central Solenoid (CS) [3]. Other projects are planning to entirely rely on the HTS technology for the whole magnet system [4]. Most of the conductor designs for such HTS coils are based on the stacked-tape concept [5] as well as on the Cable-In-Conduit Conductor (CICC) layout, developed for Low Temperature Superconductors (LTS), see two examples in Fig. 1.

In tokamaks, a subset of the coils, such as the CS coil, need to operate in time-varying magnetic field and current, thus AC losses are generated in the coils themselves. The main contribution to the total AC losses in a cable is given by the sum of the coupling and hysteresis losses. Here we call hysteresis losses those generated by current loops in the superconductor only, while we call coupling losses the ones generated by current loops that close from a superconducting region to another, through the normal conducting matrix present in the conductors. For completeness, the remaining contribution to the total AC losses is given by the eddy current losses which are generated by current loops in normal conducting materials and they are typically smaller than the other two contributions, thus they are neglected in the present work.

The associate editor coordinating the review of this manuscript and approving it for publication was Lei Zhao.

So far, the analysis of the performance of coils for fusion applications, employing HTS conductors, have considered only the coupling loss contribution [6], which have been measured for few conductors. However, it has been shown, using analytical formulae, that the contribution of the hysteresis and fully coupled losses is not negligible and, up to relatively high sweep rate (few T/s), they overcome the coupling losses [7]. This is a peculiar feature of HTS conductors which are composed of wide (few mm) tapes. Instead, for LTS conductors and coils employed in similar contexts the opposite is typically true, i.e., coupling losses are typically larger than hysteresis ones [8] already at few tens of mT/s, because the superconducting strands are composed of fine superconducting filaments (each with a diameter of few tens of micron).

Therefore, it is of paramount importance, before assessing the performance of a coil in terms of, e.g., temperature margin with thermal-hydraulic codes, to first assess the expected AC loss deposition and in particular the hysteresis loss contribution which can be large in HTS conductors.

To the aim of quantifying hysteresis losses in HTS conductors, strong effort has been put in the modelling of tapes and stack of tapes using several numerical methods as well as formulation of the Maxwell equations, such as those based on the magnetic vector potential A- and A-V formulation [9], the current vector potential, called T-A formulation, see [10], [11], [12] or the well-established H-formulation [13], see the reviews in [14] and [15] for a comprehensive overview.

Nevertheless, the electro-magnetic (EM) modelling in fusion-relevant conductors is still limited and it was focused mainly on DC performance to estimate the current distribution at the conductor terminations [16], [17] or including just few tapes [18], making hard the up-scaling of the model to conductors made of few stacks with tens of tapes, for a total of few hundreds of tapes. Therefore, due to the lack of a quantitative assessment of the hysteresis losses in a fusion-relevant context, the actual impact of those losses in HTS coil for fusion has not been quantified yet with detailed models. In turn, the effect of those losses on the performance of coils wound with HTS conductors has not been quantified yet.

In this work, we aim at computing the temperature margin reduction during the operation of the hybrid EU DEMO CS due to the presence of hysteresis losses. To this aim, we first adopted an EM numerical model based on the finite element method (FEM) and on the H-formulation to estimate the hysteresis losses in large scale conductors, focusing on the concept proposed by Swiss Plasma Center (SPC) [19], see Fig. 1(a). Having quantified the evolution of the losses during the operation of the coil, a thermal-hydraulic (TH) model of the EU DEMO CS is used to compute the evolution of the temperature margin, taking as input the losses computed by the EM model in the previous step.

The work is organized as follows: in Section II a brief description of the coil and conductors under study is
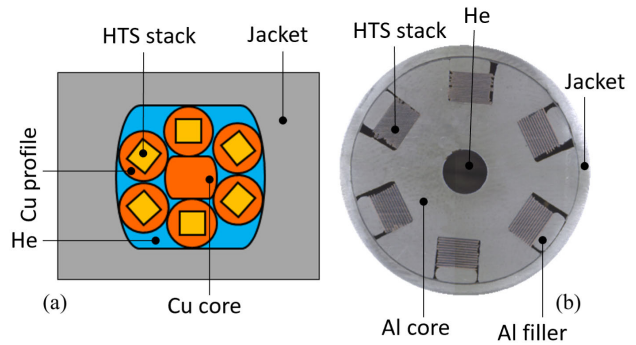

FIGURE 1. Cross-section of HTS conductor concepts proposed by (a) SPC and (b) ENEA. The main sub-elements of conductors are also indicated.

provided. In Section III, the EM model developed for a DEMO-relevant conductor and the hysteresis losses computed during the operational plasma scenario, i.e., the evolution of the currents in the tokamak coils and specifically the CS, are presented. In Section IV, the thermal-hydraulic model of the coil is described and the results -in terms of temperature margin reduction due to AC losses- are commented. In Section V, an alternative conductor concept is analyzed both in terms of losses and temperature margin, highlighting possible room for optimization of such proposal.

II. THE HYBRID EU DEMO CS

The EU DEMO CS is composed by a stack of 5 modules, see Fig. 2. The hybrid option of the EU DEMO CS features a grading of the conductors, i.e., the conductor layout may change in different layers. This is done in order to optimize the superconductor material with respect to the desired performance [3]. Therefore, the first layers (see Table 1 for their operating conditions), which are at a higher field, are designed to be wound with HTS conductors, while the remaining layers are wound with LTS conductors (Nb_3Sn or NbTi, depending on the magnetic field). Each layer is cooled in parallel to the others by a forced flow of supercritical helium entering at 4.5 K and 6 bar. The HTS conductor chosen as a case study for the present work is based on the design proposed by SPC [19] and it is composed by 6 HTS strands, each of which is made of a stack of 30 tapes, enclosed in a copper profile. The strands are then twisted around a pure copper core and inserted in a stainless-steel jacket. The voids between the twisted cable and the jacket allows for the forced flow of supercritical helium, see Fig. 2. The Nb_3Sn layers are wound with a Cable-In-Conduit Conductor (CICC) made of a bundle of superconducting and pure copper strands. Additional copper stabilizer is added with pure copper strands on top and bottom of the bundle. A separate channel, delimited by a stainless steel conduit allows for the reduction of the hydraulic impedance in the He flow. The bundle is then inserted in a stainless steel jacket. The areas of the conductor sub-elements are summarized in Table 2. The NbTi layers are not of interest for the present study since the analysis is focused on the high field layers.
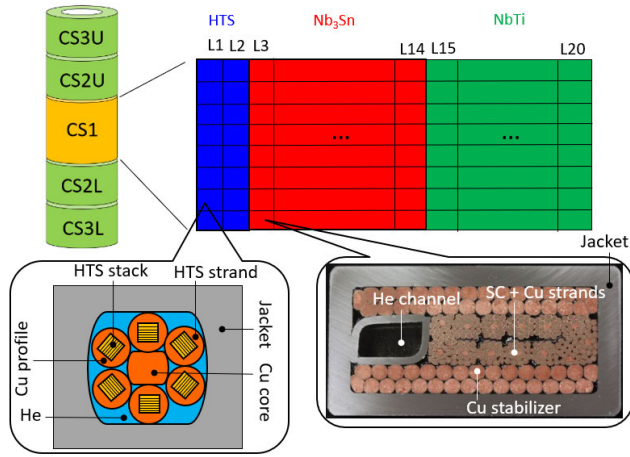
FIGURE 2. Sketch of the hybrid options of the EU DEMO CS. The schematic cut-view of the CS1 module is shown, highlighting the presence of both HTS and LTS layers. The cross-section of the HTS and LTS (Nb$_3$Sn) conductors is shown, describing all their key sub-elements.

TABLE 1. Characteristics and operating conditions foreseen in layers L1, L2 and L3 of CS1 [3].

	L1	L2	L3
Operative current (I$_{op}$) [kA]	46.3	46.3	46.3
Hydraulic length [m]	739	775	810
Maximum magnetic field (B$_{max}$) [T]	15	14.2	13.5
T$_{op}$ [K]	4.5	4.5	4.5
Turn insulation thickness [mm]	3	3	3
I$_C$(T$_{op}$, B$_{max}$) [kA]	59.7	61.9	79.2
T$_{CS}$(J$_{op}$, B$_{max}$) [K]	12.7	13.8	6.54

TABLE 2. Characteristics of the conductors in the high and medium field of the hybrid EU DEMO CS.

	L1-L2	L3-L14
Superconducting material	REBCO	Nb$_3$Sn
A$_{Cu}$ [mm^2]	480	393
A$_{SC}$ [mm^2]	1.7	110
A$_{SS}$ [mm^2]	4550	4261
A$_{He}$ [mm^2]	139	197

The EU DEMO CS is a pulsed coil, thus the transport current in the coil is expected to vary according to a given scenario to produce the desired magnetic flux. The magnetic field seen by the conductors in the CS is mainly its self-field, thus driven and determined by its current. The evolution of the magnetic field in layer L1 is reported in Fig. 3: the coil is charged in 500 s from 0 to the maximum magnetic field (here equal to 15 T); after that a fast magnetic field variation (0.75 T in 0.8 s), call "breakdown", the coil is discharged to −2.5 T in 80 s to ramp up the plasma current and to −15 T in 2 hours, i.e. the duration foreseen for the plasma burn. The coil is then discharged from −15 T to 0 T in 100 s to start another cycle or period. From this, it is clear that the main heat load in the CS is due to AC losses: depending on the conductor and on the phase of the scenario, hysteresis losses may prevail over coupling losses (see the discussion in Section III-B).
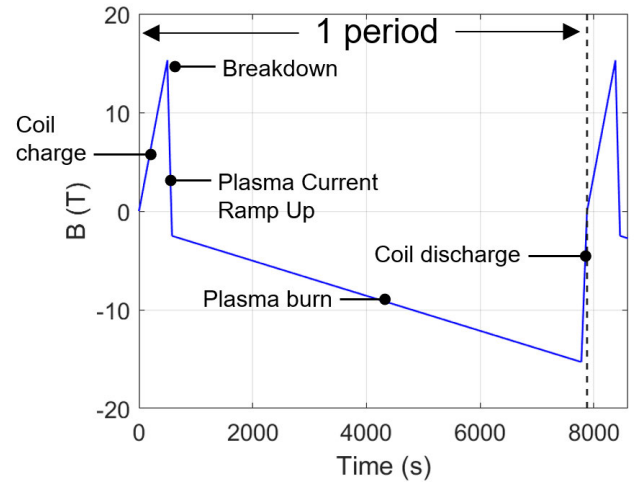

FIGURE 3. Evolution of the magnetic field in the first layer during the normal operation of the EU DEMO CS. The key phases of the scenario are highlighted.

III. ELECTRO-MAGNETIC MODEL

A well-known technique to simulate electro-magnetic transients in HTS tapes is the H-formulation implemented in FEM solvers, see the review on the H-formulation in [20]. This formulation is very well documented in literature, it can account for different tape/stack geometries and arrangements, it is robust from the point of view of numerical convergence and, provided that techniques to reduce the computational cost are employed (as discussed below in this section), it is efficient in terms of computational time. In the present work, the H-formulation is implemented in the commercial software COMSOL Multiphysics® [21].

The aim of the EM model is to compute the hysteresis losses in DEMO relevant conductors as well as operating conditions. Most of the conductors proposed so far for high field, high current applications in fusion coils are based on stack of tapes. Therefore, the first step to build an EM model for those conductors is to be able to simulate stacked tapes, possibly in a computationally efficient way. Thus, the preliminary step is to select the most efficient (and reliable way) to simulate such stack of HTS tapes.

As mentioned, the computations with the H-formulation in FEM solvers could be boosted using dedicated techniques, such as the so-called homogenization. This strategy was presented in [22] and it has been employed in several other works. Other more recent techniques have been proposed, e.g., densification, see [23].

A. EM MODEL EQUATION, SETUP AND PARAMETERS

The governing equation, written in terms of the variable **H**, can be simply derived from Maxwell equations and it is reported in (1)

$$\mu_0 \frac{\partial H}{\partial t} + \nabla \times (\rho \nabla \times H) = 0 \qquad (1)$$

TABLE 3. Parameters used in EM model used for the HTS conductor of the EU DEMO CS coil.

Parameter	Value
E_C [V/m]	10^{-4}
J_{C0} [A/m^2]	$5.2 \cdot 10^{12}$
k [-]	0.257
α [-]	0.7
B_0 [mT]	42.7
n-value [-]	27
Stack dimension [mm^2]	3.3×3.3
HTS layer thickness [μm]	1
Number of tapes per stack [-]	30

where μ_0 is the vacuum permeability, **H** is the magnetic field intensity and ρ is the electric resistivity. The resistivity of the HTS material is derived from the E-J power-law relation and it is defined as in (2)

$$\rho = \frac{E_C}{J_C(B)} \left(\frac{J}{J_C} \right)^{n-1} \tag{2}$$

where E_C critical electric field, J_C is the critical current density, B is the magnetic field induction (called magnetic field for brevity in the following), J is the current density.

The dependence of the critical current density on the magnetic field and on its orientation is taken into account according to (3)

$$J_C = \frac{J_{C0}}{\left(1 + \frac{\sqrt{k^2 B_\parallel^2 + B_\perp^2}}{B_0} \right)^\alpha} \tag{3}$$

where $B_\parallel$ and $B_\perp$ are the parallel and perpendicular component of the magnetic field to the HTS layer, respectively, and k is the anisotropy coefficient.

The stack and tape parameters used in the EM simulations are summarized in Table 3. The value of J_{C0} has been chosen to fit the conductor performance, while the other parameters are taken from other analyses performed on REBCO stacks, because measured data of these parameters for the conductor under analysis are not currently available. Nevertheless, the aim of employing a relation as (3) is to account - at least qualitatively - for the dependence of J_C on the magnetic field orientation in the calculation of the hysteresis losses.

All the simulations are carried out using a 2D domain, which corresponds to the cross section of the stack(s) (plus the surrounding air domain). This is possible as the inner radius of the EU DEMO CS is around 2 m, thus the conductor can be considered straight in this analysis. The 3D nature could play a role, in principle, when the twisting of the stack is present. To take into account the presence of the twisting the following strategy, based on analytical considerations, is adopted. The power computed in each strand is scaled according to the ratio $Q_{twisted}/Q^\theta_{untwisted}$, where $Q_{twisted}$ is the average energy deposited over one twist pitch. The latter is well approximated as $Q_{twisted} \approx \frac{4}{\pi} J_C B w$, where w is the width of the ceramic layer (almost the same as the tape width); $Q^\theta_{untwisted}$ is the energy deposited in a tape with inclination θ between the magnetic field and the wide side of the tape and it is equal to $Q^\theta_{untwisted} = 2d J_C B \cos\theta + 2w J_C B \sin\theta$, where d is the thickness of the ceramic layer (few microns), see [5] for the derivation. Therefore, in case the losses are computed with a 2D model of a stack whose tapes have the wide side that has an inclination $\theta = 60°$ with respect to the magnetic field, then the scaling factor is $\frac{4}{\pi} \cdot \frac{1}{\sqrt{3}} \approx 0.73$ (having neglected the contribution to the losses of the term corresponding to the short side of the tape, which is typically much smaller than the wide side). This strategy allows keeping the problem in 2D, taking nonetheless into account the effects of a 3D geometry.

The homogenization strategy adopted here is based on the homogenization of the critical current and it is performed scaling the critical current of the tapes to that of the stack, multiplying the tape current density by a geometric factor equal to $n_{tapes} \cdot t_{tape}/t_{stack}$, where n_{tapes} is the number of tapes in the stack, t_{tape} and t_{stack} is the thickness of the superconducting layer of one tape and that of the stack, respectively. Several benchmarks have been performed to qualify the EM model and they are reported and discussed in detail in Appendix A.

B. EM RESULTS: LOSSES IN A 6-SQUARE STACK CONDUCTOR

Once the benchmarks needed to check the reliability of the building block of the model, i.e., the model of a (tilted) stack, as well as the strategy to account for their interaction have been checked, the losses in the actual conductor can be finally computed. In Fig. 4, the evolution of the total losses in the HTS conductor reported in Fig. 2, split in the hysteresis and coupling contributions are reported. The coupling losses are computed according to (4)

$$P_{coupling} = \frac{n\tau}{\mu_0} \cdot S \cdot \left(\frac{dB}{dt} \right)^2 \tag{4}$$

where $n\tau$ is the single coupling time constant (=75 ms) [6], S is the cross-section of the cable, i.e., excluding jacket and helium (=481.7 mm^2), B is the magnitude of the magnetic field in a given point of the conductor. Equation (4) has been developed for a single stage conductor, for example filaments in a strand or stacks in a cable, and it does not work always well for multistage (4 or 5 stages) conductors, when multiple n-values should be used. Nevertheless, it was found matching well the measured values in a conductor similar to the layout analyzed here [24]. It is worth noticing that the EM model developed in this work can account for different layouts of a TSTC-like conductor (number of stacks, their orientation etc.) to quantify the hysteresis losses for a given external magnetic field. It cannot quantify the coupling losses, for which other models or measurements (as in this case) should be employed to get the overall AC loss. For the sake of completeness, it is worth highlighting that the hysteresis losses are computed without considering the presence of the transport

current, which can have a (small) impact on the hysteresis losses, as discussed in Appendix A-B. Another limitation of the present model is that it is not yet validated against measured data; however, the comparison against available analytical formulae shown in Appendix A-B is encouraging. Current work is undergoing in validating the model against experimental data to further qualify the modeling approach presented here.

The hysteresis and coupling losses have been calculated for the field profile in Fig. 4(top), which is the present scenario for the DEMO CS. It is evident from Fig. 4 that the hysteresis losses are the main contribution to the heat deposited during the CS current scenario. The only exception is the 0.8 s long "breakdown" phase where there is a steep field ramp, thus leading to large coupling losses, see Fig. 4(bottom). Apart from that very short phase, the hysteresis losses are orders of magnitude larger than the coupling, reaching tens of W/m for hundreds of seconds. In particular, the three ramps in which the magnetic field spans from -15 T to 0 T (coil discharge from the previous cycle), from 0 T to 15 T (subsequent coil charge) and from 15 T to -2.5 T (plasma current ramp up, PCRU) leads to large losses because the external field is of the order of the penetration field. In addition, as it will be confirmed in the next section, since all these ramps are contiguous, i.e., with no current flattop between them, the temperature of the coil will raise continuously, without the possibility to cooldown before the next ramp. Note that the second cycle is reported and analyzed here, because the losses become periodic after the first cycle, thus it is representative of all the subsequent ones. Furthermore, according to the discussion in Section A-B, in the first cycle, as the conductor is virgin, lower losses are computed, thus analyzing the first cycle only would lead to an underestimation of the heat deposition.

In order to account for the saturated state, the transient is simulated starting from the virgin state, i.e., at t = 0 s in the inset of Fig. 4, throughout the point where the losses become periodic, which, in this case, is after the second PCRU. A more efficient way, in case only the periodic losses are of interest, could be to start the simulation from the fully saturated state, e.g., before the start of the coil discharge.

IV. THERMAL-HYDRAULIC MODEL

The thermal-hydraulic (TH) model adopted in order to quantify the temperature margin and its results are presented in this section. The minimum temperature margin is defined as $\Delta T_{min}^{mar} = T_{CS} - T_{Co}$, where T_{CS} and T_{Co} are the current sharing temperature and the conductor temperature, respectively. This quantity is used to quantify how safe is the operation of the coil. For the EU DEMO coils, the threshold is set - at least for the LTS (sub-)coils - at 1.5 K [2]. Thermal-hydraulic models are typically employed in order to quantify the temperature margin distribution and evolution throughout the operation of the coil, in particular to estimate the
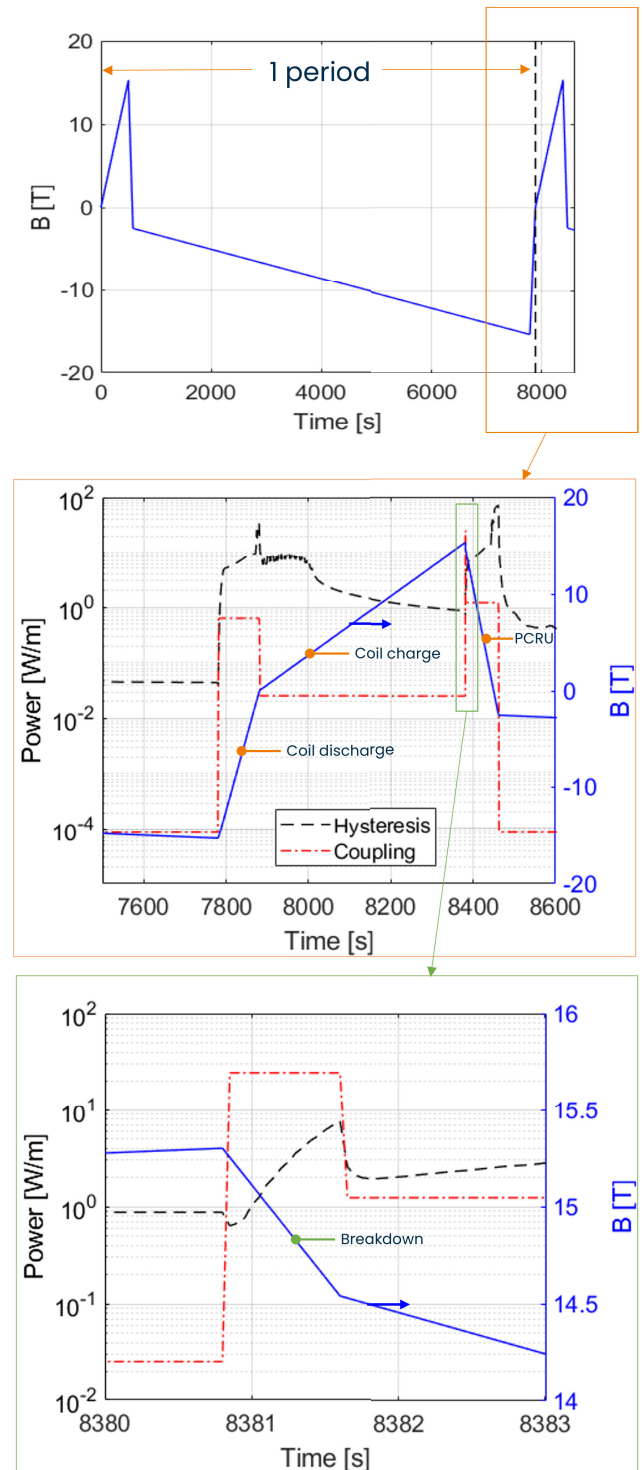

FIGURE 4. (Top) Evolution of the magnetic field during an entire plasma pulse at half the length of the EU DEMO HTS layer. (Center) Evolution of the hysteresis and coupling losses for the 6-square stack conductor during the coil discharge, charge and plasma current ramp up. (Bottom) Zoom of the breakdown phase.

distribution and evolution of the conductor temperature, which is determined by the heat deposition in the conductor and it is tightly linked to the coolant flow.

A. TH MODEL EQUATIONS, SETUP AND PARAMETERS

One-dimensional models are typically employed to perform this computations. Here, the H4C code [25], which was recently validated against quench experiments in HTS conductors [26], is adopted. It solves the 1D heat conduction equation in the solids (5); a set of 1D Euler-like partial differential equations for the coolant speed, pressure and temperature (6a-6c); a 1D diffusion-like equation for the current (7). An arbitrary number of fluid, thermal and electric regions can be simulated, depending on how the cross-section of the conductor is discretized.

Furthermore, the H4C code can take into account the heat transfer between adjacent turns and layers, which takes place through the inter-turn/inter-layer insulation. This phenomenon is particularly relevant in the case analyzed here, because the heat deposited due to AC losses in the HTS layers and in the LTS layers is quite different, thus the heat transfer between the HTS and the LTS layers cannot be neglected a priori.

$$C\frac{\partial T_i}{\partial t} - \frac{\partial}{\partial x}\left(kA\frac{\partial T_i}{\partial x}\right) = q_{s_i \leftrightarrow s_{all \neq i}} + q_{s_i \leftrightarrow f_j} + q_{J,i} + q_{AC,i}$$

(5)

$$\frac{\partial v_j}{\partial t} + v_j\frac{\partial v_j}{\partial x} + \frac{1}{\rho_j}\frac{\partial p_j}{\partial x} = 0$$

(6a)

$$\frac{\partial p_j}{\partial t} + v_j\frac{\partial p_j}{\partial x} + (\rho c^2)_j\frac{\partial v_j}{\partial x} - 2(\phi \rho f v^2)_j = \frac{\phi_j}{A_j}q_{f_j \leftrightarrow s_i}$$

(6b)

$$\frac{\partial T_j}{\partial t} + v_j\frac{\partial T_j}{\partial x} + \phi_j T_j\frac{\partial v_j}{\partial x} - 2(f v^2)_j\frac{|v_j|}{(c_v D_h)_j} = \frac{q_{f_j \leftrightarrow s_i}}{(c_v \rho A)_j}$$

(6c)

$$\left(\overline{\overline{G}}\,\overline{\overline{L}}\right)\frac{\partial I_k}{\partial t} + \frac{\partial^2 I_k}{\partial x^2} + \left(\overline{\overline{G}}\,\overline{\overline{R}}\right) \cdot I_k = 0$$

(7)

where T_i is the temperature of the i-th solid region, C its heat capacity, k its thermal conductivity, A its cross-section, $q_{s_i \leftrightarrow s_{all \neq i}}$ is the power per unit length exchanged with other solid regions (e.g., between adjacent jackets to account for inter-turn/inter-layer thermal coupling, assuming that the insulation is a simple 0D thermal resistance), $q_{s_i \leftrightarrow f_j}$ is that exchange with fluid regions, $q_{J,i}$ is the power due to Joule deposition and $q_{AC,i}$ the power per unit length deposited by AC losses, which, in this analysis is taken from the results reported in Section III-B; v_j, p_j and T_j are the velocity, pressure and temperature of the j-th fluid region, ρ, c, ϕ and c_v are the fluid density, speed of sound in the fluid, Gruneisen parameter and specific heat at constant volume, f and D_h are the friction factor and hydraulic diameter, respectively; I_k is the current in the k-th electric element, $\overline{\overline{G}}\,\overline{\overline{L}}$ is the product of the matrix of the (linear) transverse resistance between electric regions in contact and their inductance, $\overline{\overline{R}}$ is the matrix with the (linear) longitudinal resistance of each electric region.

In the case at hand, the TH model implemented in the H4C code is sketched in Fig. 5. The coolant is supercritical
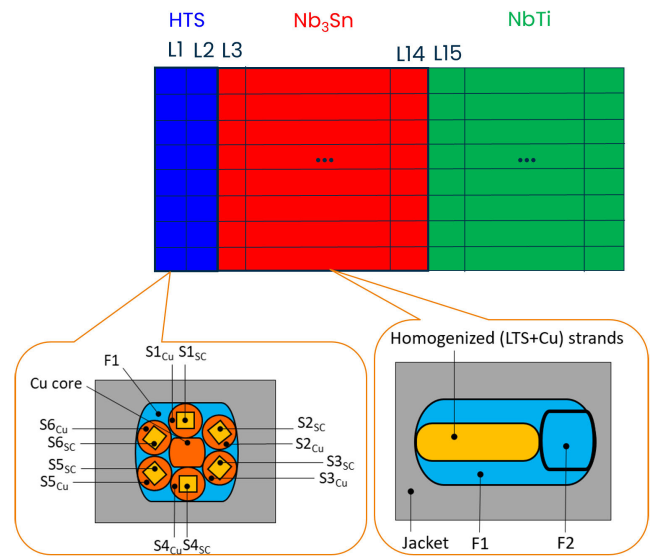

FIGURE 5. Cross-section of the proposed hybrid (HTS-LTS) CS coil for the EU DEMO. In the insets, the sketch of the discretization of the conductor cross-section used in the TH model for the HTS and LTS conductor is reported.

TABLE 4. Parameters for the REBCO and Nb$_3$Sn scaling used in the TH analysis.

Parameter	REBCO	Nb$_3$Sn
T_{c0m} [K]	90	16.48
B_{c20m} [T]	132.5	23.9
A [A·T/m^2]	$1.464 \cdot 10^8$	$8.077 \cdot 10^{10}$
p [-]	0.5875	0.556
q [-]	1.7	1.698
α [-]	1.54121	-
β [-]	1.96679	-
ϵ [%]	-	-0.00250
ϵ_n [-]	-	$-6.41 \cdot 10^{-4}$
ϵ_{0a} [-]	-	$2.32 \cdot 10^{-3}$
C_{a2} [-]	-	4.431
C_{a1} [-]	-	45.74

helium at the initial conditions of 4.5 K and 6 bar. Different discretization strategies have been adopted for the HTS and LTS layers. A similar setup was already presented and used for quench analysis in [27].

As we are interested primarily in computing the conductor temperature as a results of the heat deposited by AC losses, the presence of the current in the conductor is neglected: this allows not having a quench during the simulation. The comparison with the T_{CS} is performed in the post-processing phase. The T_{CS} is computed from the given scaling law of the J_C of the superconductor under analysis (in this case REBCO and Nb$_3$Sn). For this, the J_C scaling needs to account also for the temperature dependence, thus the scaling law reported in [28] and [29] are considered for REBCO and Nb$_3$Sn, respectively. The parameters of the scaling laws are reported in Table 4 and they are taken from [28] and [30] for the HTS and LTS conductors, respectively.
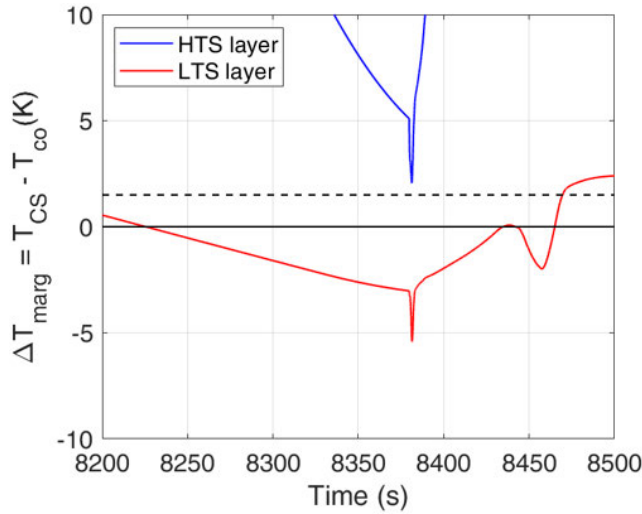
FIGURE 6. Evolution of the minimum temperature margin in both HTS and LTS layers of CS1.

(a)

(b)

FIGURE 7. Evolution of the conductor temperature obtained with the TH model using as input the losses computed with the FEM model (black curve) and with the analytical formulae for the slab (blue curve) in the (a) HTS and (b) LTS conductors of the CS3U module. The evolution of the corresponding T_{CS} is also reported.

B. TH RESULTS: TEMPERATURE MARGIN

The temperature margin evolution in both the first HTS layer and the first LTS layer is shown in Fig. 6. The discussion is focused on those layers because they are at the highest magnetic field, for the HTS and LTS sub-coil, respectively. It is shown that the margin in the HTS layer is positive, although it is much lower than that computed, for example, in [6], where the hysteresis losses in the HTS conductor are neglected and the minimum margin was computed to be around 5 K. Including the hysteresis loss contribution, a minimum margin around 2 K is found, see Fig. 6. However, the main issue in the proposed design appears to be the heat transfer from the HTS layers to the LTS ones: while the large T_{CS} in the HTS conductor is able to compensate the large T_{Co} reached due to the heat deposition by AC losses, the additional heat coming from the HTS to LTS layers is too large to be compensated by the T_{CS} in the LTS conductor (this is confirmed by a separate simulation carried out without thermal coupling between the HTS and LTS layers, where the temperature margin is above 2 K in the first LTS layer, as also shown in [6]). The result is that the temperature margin in the LTS layers becomes negative (up to -5 K), thus it would lead to quench in the LTS layers as soon as the second cycle is performed. Note that the temperature margin in the first LTS layer before the coil discharge (at t = 7780.8 s), i.e., when the heat deposition in HTS layers is low, thus the heat reaching the LTS layers is also low, reaches a minimum of 1.9 K (not shown in Fig. 6). The feedback of the temperature evolution on that of the hysteresis losses is discussed in Appendix B.

Concerning the modelling approach, it is useful to directly compare the TH results obtained with the hysteresis losses computed with the EM model of Section III with those obtained with the analytical formulae discussed in Appendix A-B. Note that the latter is the typical approach
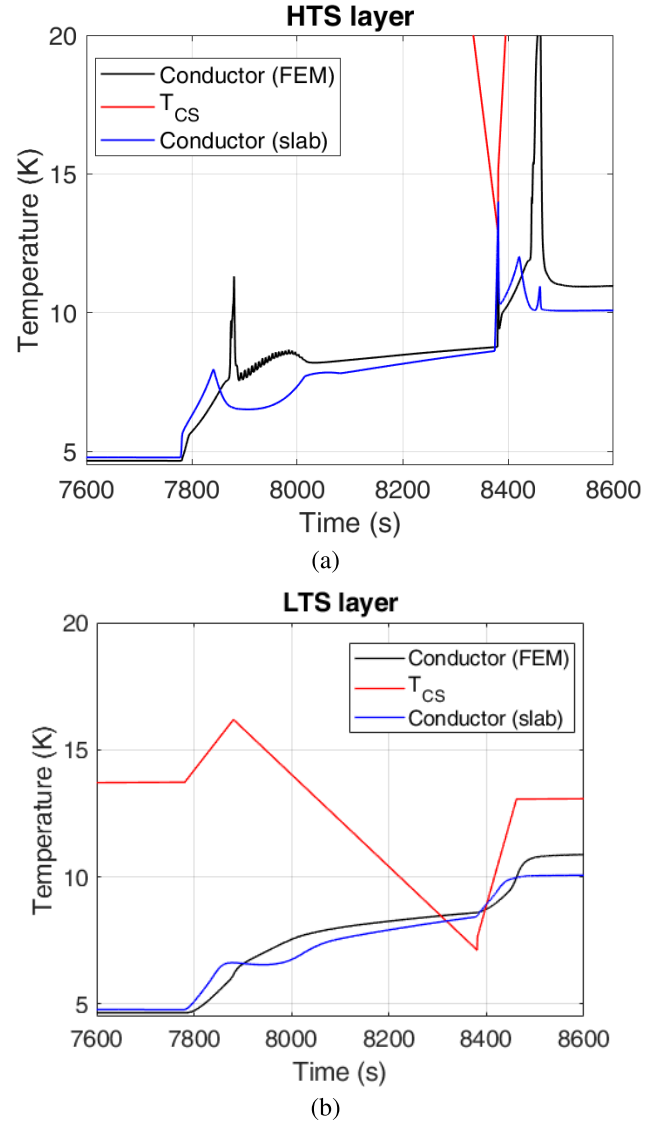
adopted for the TH analysis of LTS coils subject to AC losses with a very good accuracy when compared to experimental results [31] and it is less time consuming because it does not need to run an EM simulation to generate the input for the TH analysis. The comparison is reported in Fig. 7. It is evident that the use of analytical formulae to compute the hysteresis losses leads to the same qualitative picture given by the use of an EM numerical model, i.e., the excessive heating reaching the LTS layers. However, the temperature peaks in the HTS conductor are not well reproduced, therefore the quantitative verification of a design should foresee the EM modelling of the losses to be then used as input for the TH calculation. Also, the use of the analytical models underestimate the total energy deposited and this could be an issue in the

verification of the heat load to be handled by the cryoplant. Therefore, given the results reported in Fig. 7, the analytical formulae can be considered a fast and reliable tool for the conductor design and optimization. However, for the design verification phase, where more detailed tools are to be used, an EM calculation is needed to provide the TH analysis with a more accurate input, because the analytical formualae are not conservative: they do not reproduce the peaks of deposited power, which in turn would lead to non negligible peaks of temperature.

V. ALTERNATIVE CONCEPT

An alternative conductor concept with respect to those based on few square stacks is the monoblock conductor proposed in [7]. The idea is to stack hundreds of tapes (180 in the case analyzed here), obtaining a single untwisted rectangular stack with large aspect ratio, e.g., 10, with the wide side parallel to the main component of the magnetic field. In this way, the hysteresis losses are negligible in the central modules where the field is basically parallel to the CS axis. On the other hand, the fully coupled losses becomes the major contribution as discussed below in this section.

The radial component of the magnetic field, thus perpendicular to the wide side of the stack, becomes no more negligible in the upper and lower modules of the CS coil, see Fig. 8a, leading to an increase of the hysteresis losses with respect to the central modules.

The EM model has been used to compute the hysteresis losses both in the central modules as well as in the upper/lower modules.

For the central modules, since the only relevant component of the field is the axial one, thus parallel to the tapes, the hysteresis losses become negligible.

However, in this configuration, the coupling losses become predominant. A first estimation of these losses has been carried out assuming that the tapes are fully coupled, i.e., assuming that the losses are in the so-called saturated regime. In this regime, the stack behaves as a bulk superconductor, thus the coupling losses have been computed assuming a simple rectangle of the same dimensions of the stack, using the same model and formulation presented in Section III. The evolution of the losses in the two concepts, in the central module (CS1) is shown in Fig. 8b, where it can be seen that these losses are comparable to those of the 6-square stack configuration, thus this alternative configuration does not bring strong advantage from the AC losses point of view.

To compute the losses in the upper/lower modules, the homogenized model of the rectangular stack is used, thus computing only the hysteresis loss contribution, imposing as boundary condition the magnetic field component as shown in Fig. 8a. The evolution shown in Fig. 8c is computed in the last turn of the first layer, i.e., where the losses in the rectangular stack are the largest. In that point, the losses are larger than those in the 6-square stack conductor. This is the consequence of having a 4 T component of the field that is
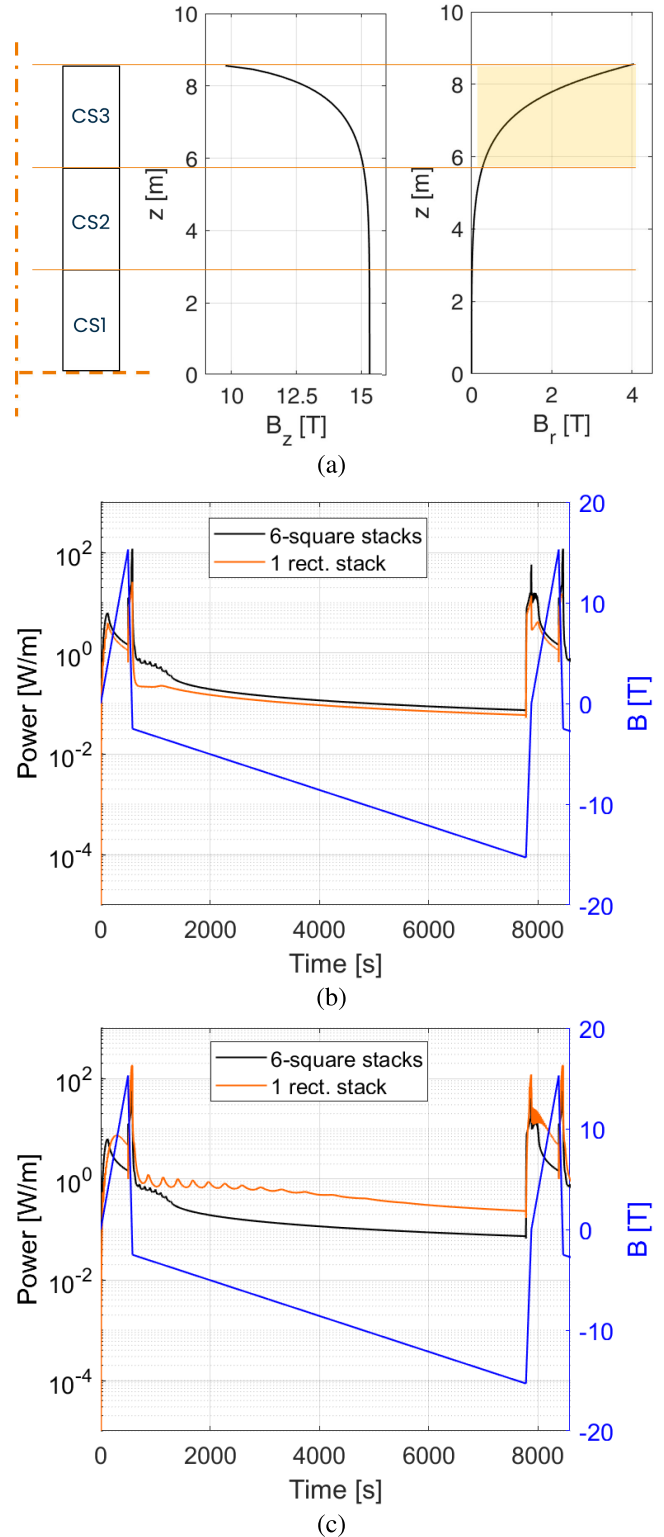

(a)

(b)

(c)

FIGURE 8. (a) Axial profile in the first layer of (half of) the CS1, CS2 and CS3 of the axial (B_z) and radial (B_r) component of the magnetic field. (b) Evolution of the losses in CS1 and (c) at the end of the first layer of CS3 in case of 6-square stack and single rectangular stack options. The external magnetic field (right axis) is also reported.

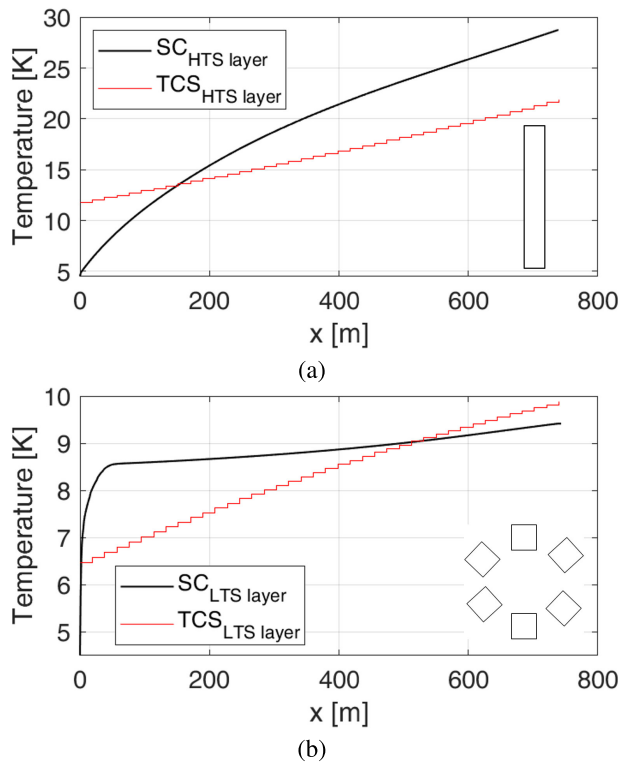perpendicular to the wide face of the tapes, leading to large hysteresis losses.

FIGURE 9. Distribution of the conductor (black line) and current sharing temperatures (red line) in the CS3 for (a) the monoblock option and for (b) the 6-square stack conductor.

The results of the computation of the temperature margin in the upper module of the CS coil (CS3U), which for symmetry behaves as the lower module (CS3L), is shown in Fig. 9 as the comparison of the conductor temperature with the current sharing temperature. In the case of the monoblock conductor, as the hysteresis losses are larger going towards the outlet, assumed to be at the top of the module, it can be seen that the conductor temperature grows following qualitatively the distribution of the T_{CS}, which grows as well towards the outlet because the magnitude of the magnetic field decreases. On the other hand, in the case of the 6-square stack conductor, where the issue is in the LTS layers, as discussed in Section IV-B, the conductor temperature grows a lot in the first meters, because the losses in the HTS layer are larger where the magnitude of the field is larger. This does not take advantage of the distribution of the T_{CS}: the larger heating, thus the larger conductor temperature is located where the T_{CS} is the lowest, while, being different the conductor design, if a monoblock conductor is considered, the losses are lower where the T_{CS} is lower and they gradually increase. Therefore, this advantage of the monoblock conductor could be a feature to be optimized. Nevertheless, at the present stage, the losses are too large to have a positive margin, already in the HTS layers.

VI. CONCLUSION AND PERSPECTIVE
Hysteresis losses in HTS conductors exposed to high and time-varying magnetic field, designed for nuclear fusion applications, have been quantified using a finite element electro-magnetic model based on the H-formulation. It was shown that the coupling losses in twisted-stack tape conductor (TSTC) give only a marginal contribution, while the hysteresis losses are orders of magnitude larger.

The impact of the losses on the temperature margin of the coil was analyzed with a thermal-hydraulic model, in the case of the EU DEMO hybrid Central Solenoid. It was observed that part of the large heat deposited due to AC losses in the HTS layers is transferred to the LTS layers, which end up in having a negative temperature margin, thus the conductor or coil design should be optimized, trying to minimize the losses in the HTS layers or improving the cooling of the high field layers.

A concept, alternative to the TSTC idea, was also analyzed both in terms of hysteresis losses as well as in terms of thermal-hydraulic performance. This concept, based on having a single monoblock conductor, leads anyway to large hysteresis losses, at least in the top and bottom modules of the CS coil, thus leading to too high conductor temperatures. Nevertheless, the concept is promising as the heat deposition becomes larger where also the current sharing temperature increases, therefore there can be room for optimization.

The electro-magnetic and thermal-hydraulic models have proven to be applicable to large scale conductors to be used in coils for nuclear fusion applications. In perspective, the EM model will be validated against experimental results and the EM+TH models will be used to explore other conductor concepts, more optimized for pulsed operation.

APPENDIX A
ELECTRO-MAGNETIC MODEL BENCHMARKS
In this appendix, the benchmarks performed on the EM model of Section III are described and discussed.

A. HOMOGENIZED MODEL
The first step is to benchmark the homogenized model of one stack of tapes with the reference model, developed with the same formulation, but simulating each superconducting layer of each tape in detail.

The comparison of the overall losses in the stack is presented in Fig. 10 and it shows that the homogenized model agrees very well with the reference model, while saving elements in the mesh, thus computational time: the relative error is in each point lower than 0.5%, except for only four points for which the error is between 10% and 15%. Nevertheless, two of these points corresponds to when the minimum losses (close to 0 W/m) are computed, thus they are not relevant, while the remaining two corresponds to the maximum. However, being just single points, they do not alter remarkably the average accuracy of the calculation. The homogenized stack shown in Fig. 10 is the building block of the final conductor model. The homogenized model, based on the H-formulation, has been also compared with a model implementing the T-A formulation and the same results have been obtained.
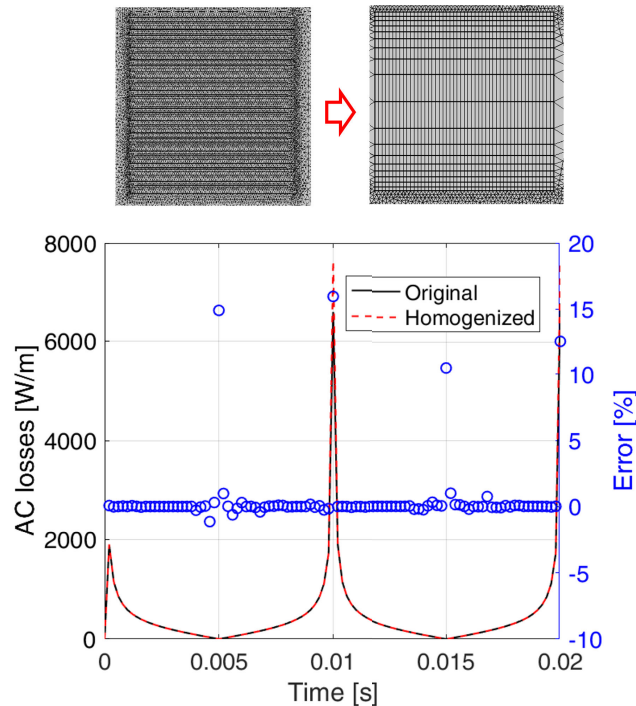
FIGURE 10. Evolution of the losses computed with a detailed model in which each tape is meshed and modelled and with the homogenized model. The relative error between the two curves is also shown. The meshes used for the two models are reported in the top, showing the decrease of the nodes going from the detailed to the homogenized model.

B. ANALYTICAL FORMULAE

There are analytical formulae to compute the hysteresis losses for various geometry. The most interesting for the case at hand are those for slab and square conductors. The first is the most investigated case, see, e.g., [32] and [33], as it is the simplest and very useful for many real case applications. Considering the geometry of interest in this work, the set of semi-analytical formulae developed for rectangular bars in [34] are also considered. The formulae for the slab in [33], page 439, provide a description of magnetic history, but the slab is a good approximation for a square only at relatively high field, say $> 2B_p$, where B_p is the penetration field. The semi-analytical formula for a square [34] are perfect for the square stack, but provide the total energy deposited in a full cycle (from 0 to B_m, to 0, to $-B_m$, to 0); only the average power can be obtained, and this would underestimate the power, especially during the ramp up at low field. The FEM analysis has two advantages with respect to analytical formulae: 1) it provides both geometrical and magnetic history descriptions, 2) it contains a finite n-value, while the analytical expressions consider a infinite n-value, since they are based on the Critical State Model [35].

The formulae are compared in Fig. 11, where 3/4 of a cycle with linear variations of the external magnetic field, is considered and the consequent power generation

due to hysteresis losses is computed. The maximum field and the duration of the magnetic field ramps are chosen because they are representative of the CS operation of the EU DEMO. In case the formulae have been developed for the computation of the energy deposition, such as in [34], the power is computed simply deriving in time the energy.

The considered models agrees in identifying the penetration field (B_p), i.e., the field above which the superconductor is fully penetrated, around 3-4 T. Nevertheless, some differences can be identified. Note that the formula for the square stack is plotted starting from t = 500 s because it is developed for a magnetized stack. On the other hand, the formulae for the slab account for the virgin state, thus they are plotted starting from t = 0 s.

For $B < B_p$, the impact of having a finite geometry, e.g., a square, is visible: the slab formulas underestimate the losses, the slab being a not so good approximation for a square stack. In this range, the FEM model results agrees very well with the square formulae. For $B > 2B_p$, the formula developed for rectangular conductors tends to that for the slab. In this field range, as the stack is fully penetrated, it can be well approximated with a slab. Indeed, the FEM model agrees very well with the red curve.

Furthermore, the set of formulae presented in [33], developed to compute the energy deposited in the slab, shows that the first ramp up, i.e., from the virgin state, leads to larger losses than the ramp down. The square formula is not able to predict this behavior, as it provides the average power during an entire cycle. Also in this case, the FEM model predicts correctly this feature, as the first peak of the blue curve is higher than the second peak at t = 950 s. This behavior, i.e., larger losses during the ramp-up than during the ramp-down, is even more evident when the second-half of the cycle is simulated. From t = 1500 s, the losses become periodic with a period equal to 1000 s. Nevertheless, the analytical formulae clearly underestimates the losses during the second ramp-up, which is a crucial phase during the charge of the EU DEMO CS.

At t = 500 s, in the case of linear magnetic field excitation, the first derivative of the field is discontinuous, therefore the analytical formulae are not defined. After t = 500 s, the analytical formulae are exactly symmetric with respect to the ramp-up phase, while the FEM model takes into account the magnetization history.

Lastly, the set of formulae available in [36] allows computing the losses in case also a transport current is present (together with an external magnetic field). The contribution of the current leads to a slight increase of the losses above the penetration field (not shown). However, since the increase is small and it would add difficulty in the convergence of the numerical model, it has been assumed no transport current in the FEM simulations.

From the comparison of the (small subset of) formulae, it is evident that the FEM model accounts for all the qualitative
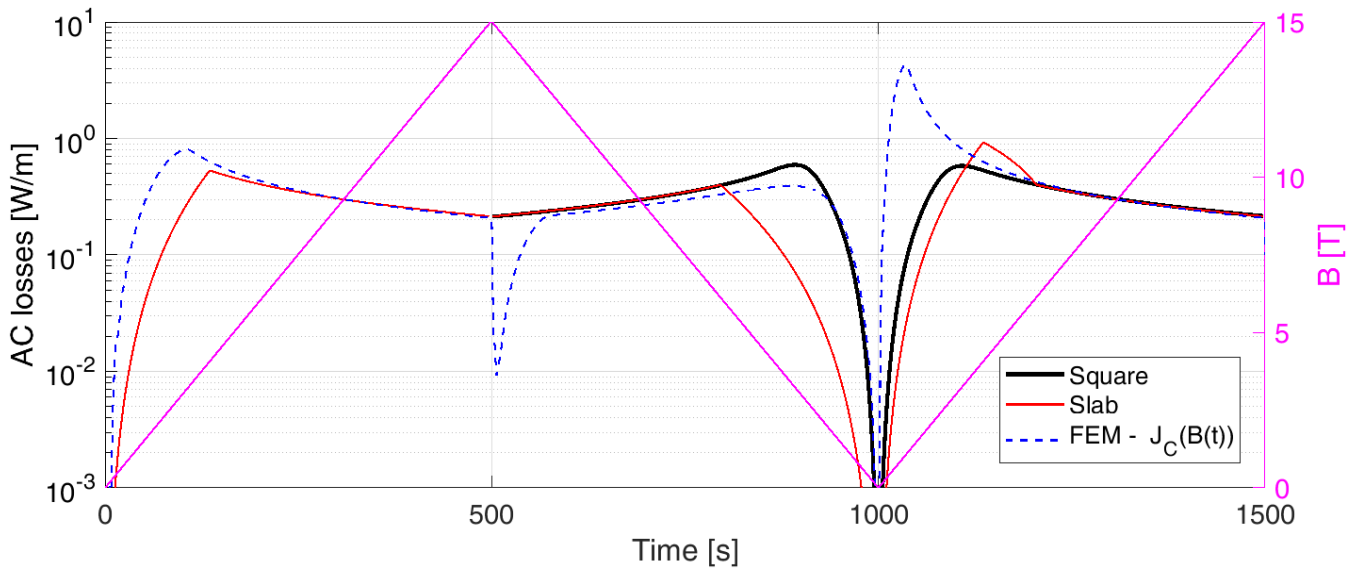
FIGURE 11. Evolution of the losses in the 3/4 of a linear cycle of an externally applied magnetic field (magenta curve) computed using different analytical formulae and compared with the FEM model presented in this work. The formula for the square stack is taken from [34] and that for the slab from [33].

features of the losses evolution shown by the analytical formulations analyzed here. In addition, the numerical model is able to account for the geometry at hand, the magnetization history and a finite n-value, which are all features that lead to a quantitative difference with respect to the analytical formulae, which cannot account for those details. The accuracy on the losses calculation is needed since a simple order of magnitude estimate can lead to too large errors on the temperature estimation. Order of magnitude estimates are fundamental during the conductor design phase, while more accurate estimation are needed when the design has to be verified with design verification tools, which are typically sophisticated numerical codes.

C. TILTED TAPES AND STACKS

In the literature, there are available few studies on the hysteresis losses in tilted tapes. Since high current conductors are typically built or designed using stack of tapes, we first benchmarked the modelling strategy for few tapes - for which literature data are available - and then we used the benchmarked tape model to, in turn, benchmark the homogenized (tilted) stack model.

The benchmark of the EM model of tilted tapes have been performed against the data available in [37]. Here, a single tape was simulated - accounting only for the superconducting layer - for different angles between the imposed external magnetic field and the c-axis of the tape. The agreement is good for all the magnetic fields for which data are available and for all the tilt angles, ranging from 0 to 90°, see Fig. 12.

It is worth highlighting that the mesh needed to model tapes with field orientation close to parallel becomes more and more demanding in terms of elements in the tape
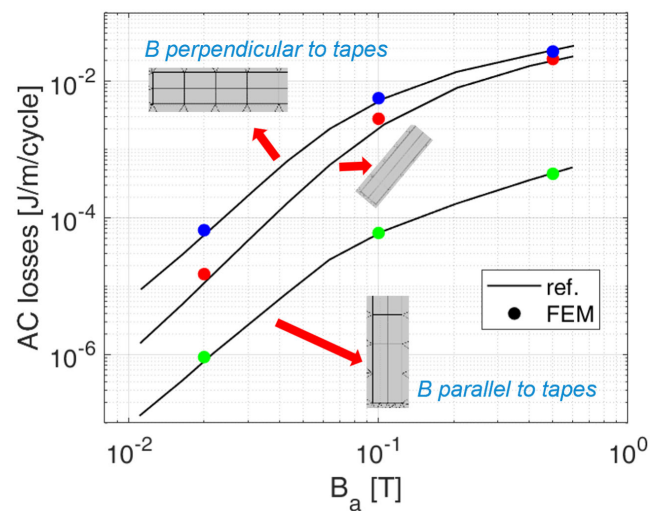

FIGURE 12. Benchmark of the energy per cycle computed with different tilt angles at different magnetic fields using the model presented here against the data reported in [37].

cross-section: for field perpendicular to the tape, only one element is sufficient, while for field parallel to the tape, at least four elements are needed to catch the correct value of the energy deposited, making the computation progressively more demanding as the field tends to be parallel to the superconducting layer.

Once the EM model is validated also for a tilted tape, the full model of a stack with 30 tapes is developed. This model was then used as reference model to benchmark the homogenized model of a tilted stack, which is, in turn, the building block of the full conductor model. The comparison of the power deposited in the stack as consequence of a sinusoidal
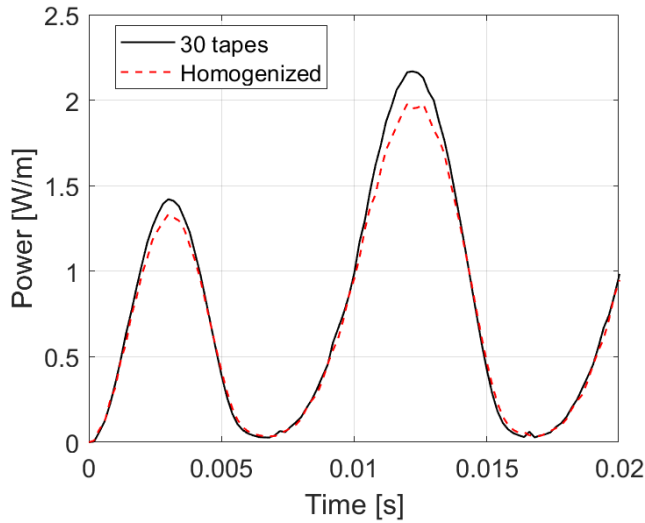
FIGURE 13. Evolution of the losses computed with a detailed model accounting for each of the 30 tapes and with the homogenized model.

FIGURE 14. Comparison of the evolution of the energy per cycle as function of the magnetic field computed accounting for the interaction between the stacks (red curve) or summing the losses of each stack simulated separately (black curve). The corresponding error using the second method is shown in blue.

field cycle, computed with the reference stack model and the homogenized one is shown in Fig. 13.

D. INTERACTION BETWEEN STACKS

To optimize the computation of losses in case of a conductor made of multiple stacks, a possible way could be to simulate only one stack at a time, with all the different orientation. This is because the simulation of a single stack is much faster and it is easier to obtain convergence than the simulation of multiple stacks together. Nevertheless, due to the amplitude of the magnetic field of interest, as well as to the distance between the stack, the interaction between them cannot be neglected, at least at magnetic field below the penetration field, i.e., 3-4 T for the case at hand. This result is visible in Fig. 14. Here, the energy per cycle deposited at different magnetic field (considering a sinusoidal cycle) obtained with two different setups is shown. In one case, two stacks are simulated together, thus accounting for the electromagnetic interaction between them; in the other, the losses obtained simulating one stack at a time are summed up. It is clear that below the penetration field, the losses in case of the simulation of single stacks are underestimated, meaning that the interaction between the stacks is not negligible and it tends to increase the losses. This is due to the shielding of the field, which tends to increase the field close to the edges of a stack, due to the shielding of the other. This effect was already known and discussed in the case of low temperature superconducting strands, see [32]. Therefore, at least below the penetration field, the stacks must be simulated all together.

APPENDIX B
EFFECT OF TEMPERATURE ON THE AC LOSSES

The EM simulations discussed in Section III were carried out at constant temperature. However, the results obtained
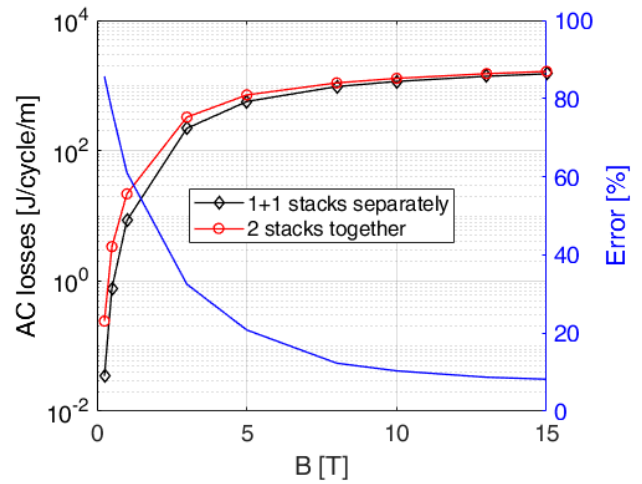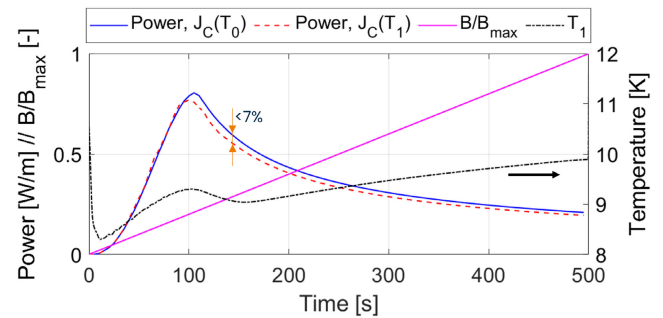

FIGURE 15. Comparison of the evolution of the losses computed with constant (T_0) or variable (T_1) temperature. The corresponding (normalized) evolution of the magnetic field is also shown.

with the TH model showed that a large temperature increase is expected in the HTS conductors, thus the losses computed with the EM model could be different if the temperature evolution throughout the transient is taken into account.

In order to estimate the impact of the temperature increase in the losses computation, a first iteration between the EM and the TH model has been performed. Note that, in principle, the two models should be coupled, as the critical current density depends also on the temperature. In the case, the strategy adopted is to loosely couple the two models in the following way: the losses (P_0) are first computed with the EM model at constant temperature T_0; the new temperature (T_1) is then computed with the TH model; the temperature (evolution) T_1 is then used as input for the losses (J_C) calculation in the EM model. The two loss evolution are plotted in Fig. 15 and it is shown that accounting for the temperature rise due to the magnetic field ramp up (from 0 to 15 T) leads to a maximum difference in the loss evolution of less than 7%. Even though the converged loss and temperature evolution

should be computed by keep iterating between the EM and the TH model, already the first iteration shows that the losses computed with a constant temperature (more precisely, a constant J_C with respect to the temperature) is very close to the losses computed with a temperature ranging from 8 K to 10 K. see again Fig. 15. Therefore, neglecting the temperature dependence of the J_C in the EM model is acceptable and it can be kept uncoupled with respect to the TH model.

ACKNOWLEDGMENT

REFERENCES

[1] P. Bruzzone, W. H. Fietz, J. V. Minervini, M. Novikov, N. Yanagi, Y. Zhai, and J. Zheng, "High temperature superconductors for fusion magnets," *Nucl. Fusion*, vol. 58, no. 10, Oct. 2018, Art. no. 103001.

[2] V. Corato et al., "The DEMO magnet system—Status and future challenges," *Fusion Eng. Des.*, vol. 174, Jan. 2022, Art. no. 112971.

[3] R. Wesche, X. Sarasola, O. Dicuonzo, I. Ivashov, K. Sedlak, D. Uglietti, and P. Bruzzone, "Hybrid HTS-Nb$_3$Sn-NbTi DEMO CS coil design optimized for maximum magnetic flux generation," *Fusion Eng. Des.*, vol. 146, pp. 10–13, Sep. 2019.

[4] B. N. Sorbom, J. Ball, T. R. Palmer, F. J. Mangiarotti, J. M. Sierchio, P. Bonoli, C. Kasten, D. A. Sutherland, H. S. Barnard, C. B. Haakonsen, J. Goh, C. Sung, and D. G. Whyte, "ARC: A compact, high-field, fusion nuclear science facility and demonstration power plant with demountable magnets," *Fusion Eng. Des.*, vol. 100, pp. 378–405, Nov. 2015.

[5] M. Takayasu, L. Chiesa, L. Bromberg, and J. V. Minervini, "HTS twisted stacked-tape cable conductor," *Supercond. Sci. Technol.*, vol. 25, no. 1, Dec. 2011, Art. no. 014011.

[6] A. Dembkowska, M. Lewandowska, and X. Sarasola, "Thermal-hydraulic analysis of the DEMO CS coil," *IEEE Trans. Appl. Supercond.*, vol. 28, no. 4, pp. 1–5, Jun. 2018.

[7] D. Uglietti, R. Kang, R. Wesche, and F. Grilli, "Non-twisted stacks of coated conductors for magnets: Analysis of inductance and AC losses," *Cryogenics*, vol. 110, Sep. 2020, Art. no. 103118.

[8] M. Breschi, L. Cavallucci, P. Bauer, F. Gauthier, R. Bonifetto, A. Zappatore, R. Zanino, N. Martovetsky, K. Khumthong, E. Ortiz, and J. Sheeron, "AC losses in the second module of the ITER central solenoid," *IEEE Trans. Appl. Supercond.*, vol. 32, no. 6, pp. 1–5, Sep. 2022.

[9] N. Nibbio, S. Stavrev, and B. Dutoit, "Finite element method simulation of AC loss in HTS tapes with B-dependent E-J power law," *IEEE Trans. Appl. Supercond.*, vol. 11, no. 1, pp. 2631–2634, Mar. 2001.

[10] H. Zhang, M. Zhang, and W. Yuan, "An efficient 3D finite element method model based on the T–A formulation for superconducting coated conductors," *Supercond. Sci. Technol.*, vol. 30, no. 2, Dec. 2016, Art. no. 024005.

[11] F. Liang, S. Venuturumilli, H. Zhang, M. Zhang, J. Kvitkovic, S. Pamidi, Y. Wang, and W. Yuan, "A finite element model for simulating second generation high temperature superconducting coils/stacks with large number of turns," *J. Appl. Phys.*, vol. 122, no. 4, Jul. 2017, Art. no. 043903.

[12] E. Berrospe-Juarez, V. M. R. Zermeño, F. Trillaud, and F. Grilli, "Real-time simulation of large-scale HTS systems: Multi-scale and homogeneous models using the T–A formulation," *Supercond. Sci. Technol.*, vol. 32, no. 6, Apr. 2019, Art. no. 065003.

[13] R. Brambilla, F. Grilli, and L. Martini, "Development of an edge-element model for AC loss computation of high-temperature superconductors," *Supercond. Sci. Technol.*, vol. 20, no. 1, pp. 16–24, Nov. 2006.

[14] F. Grilli, E. Pardo, A. Stenvall, D. N. Nguyen, W. Yuan, and F. Gömöry, "Computation of losses in HTS under the action of varying magnetic fields and currents," *IEEE Trans. Appl. Supercond.*, vol. 24, no. 1, Feb. 2014, Art. no. 8200433.

[15] L. Quéval, V. M. R. Zermeño, and F. Grilli, "Numerical models for AC loss calculation in large-scale applications of HTS coated conductors," *Supercond. Sci. Technol.*, vol. 29, no. 2, Jan. 2016, Art. no. 024007.

[16] V. Zermeno, P. Krüger, M. Takayasu, and F. Grilli, "Modeling and simulation of termination resistances in superconducting cables," *Supercond. Sci. Technol.*, vol. 27, no. 12, Nov. 2014, Art. no. 124013.

[17] G. De Marzi, G. Celentano, A. Augieri, M. Marchetti, and A. Vannozzi, "Experimental and numerical studies on current distribution in stacks of HTS tapes for cable-in-conduit-conductors," *Supercond. Sci. Technol.*, vol. 34, no. 3, Feb. 2021, Art. no. 035016.

[18] F. Grilli, V. M. R. Zermeño, and M. Takayasu, "Numerical modeling of twisted stacked tape cables for magnet applications," *Phys. C, Supercond. Appl.*, vol. 518, pp. 122–125, Nov. 2015.

[19] D. Uglietti, R. Wesche, and P. Bruzzone, "Design and strand tests of a fusion cable composed of coated conductor tapes," *IEEE Trans. Appl. Supercond.*, vol. 24, no. 3, pp. 1–4, Jun. 2014.

[20] B. Shen, F. Grilli, and T. Coombs, "Review of the AC loss computation for HTS using H formulation," *Supercond. Sci. Technol.*, vol. 33, no. 3, Feb. 2020, Art. no. 033002.

[21] COMSOL. (2021). *COMSOL Multiphysics 5.6*. [Online]. Available: https://www.comsol.com

[22] V. M. R. Zermeno, A. B. Abrahamsen, N. Mijatovic, B. B. Jensen, and M. P. Sørensen, "Calculation of alternating current losses in stacks and coils made of second generation high temperature superconducting tapes for large scale applications," *J. Appl. Phys.*, vol. 114, no. 17, Nov. 2013, Art. no. 173901.

[23] E. Berrospe-Juarez, F. Trillaud, V. M. R. Zermeño, and F. Grilli, "Advanced electromagnetic modeling of large-scale high-temperature superconductor systems based on H and T–A formulations," *Supercond. Sci. Technol.*, vol. 34, no. 4, Feb. 2021, Art. no. 044002.

[24] N. Bykovsky, D. Uglietti, R. Wesche, and P. Bruzzone, "Cyclic load effect on round strands made by twisted stacks of HTS tapes," *Fusion Eng. Des.*, vol. 124, pp. 6–9, Nov. 2017.

[25] A. Zappatore, R. Heller, L. Savoldi, M. J. Wolf, and R. Zanino, "A new model for the analysis of quench in HTS cable-in-conduit conductors based on the twisted-stacked-tape cable concept for fusion applications," *Supercond. Sci. Technol.*, vol. 33, no. 6, May 2020, Art. no. 065004.

[26] A. Zappatore, R. Bonifetto, P. Bruzzone, V. Corato, O. Dicuonzo, M. Kumar, K. Sedlak, and B. Stepanov, "Quench experiments on sub-size HTS cable-in-conduit conductors for fusion applications: Data analysis and model validation," *Cryogenics*, vol. 132, Jun. 2023, Art. no. 103695.

[27] A. Zappatore, R. Bonifetto, X. Sarasola, and R. Zanino, "Effect of local defects on HTS fusion magnets performance," *IEEE Trans. Appl. Supercond.*, vol. 32, no. 5, pp. 1–9, Aug. 2022.

[28] R. Heller, P. V. Gade, W. H. Fietz, T. Vogel, and K.-P. Weiss, "Conceptual design improvement of a toroidal field coil for EU DEMO using high-temperature superconductors," *IEEE Trans. Appl. Supercond.*, vol. 26, no. 4, pp. 1–5, Jun. 2016.

[29] L. Bottura and B. Bordini, "$J_C(B, T, \varepsilon)$ parameterization for the ITER Nb$_3$Sn production," *IEEE Trans. Appl. Supercond.*, vol. 19, no. 3, pp. 1521–1524, Jun. 2009.

[30] N. Martovetsky, T. Isono, D. Bessette, A. Devred, Y. Nabara, R. Zanino, L. Savoldi, R. Bonifetto, P. Bruzzone, M. Breschi, and L. Zani, "Characterization of the ITER CS conductor and projection to the ITER CS performance," *Fusion Eng. Des.*, vol. 124, pp. 1–5, Nov. 2017.

[31] A. Zappatore, R. Bonifetto, N. Martovetsky, and R. Zanino, "Validation of the 4C code on the AC loss tests of a full-scale ITER coil," *IEEE Trans. Appl. Supercond.*, vol. 33, no. 5, pp. 1–5, Aug. 2023.

[32] M. Wilson, *Superconducting Magnets*. New York, NY, USA: Oxford, 1992.

[33] Y. Iwasa, *Case Study in Superconducting Magnet Design*. New York, NY, USA: Springer, 2009.

[34] E. Pardo, D.-X. Chen, A. Sanchez, and C. Navau, "The transverse critical-state susceptibility of rectangular bars," *Supercond. Sci. Technol.*, vol. 17, no. 3, pp. 537–544, Feb. 2004.

[35] C. P. Bean, "Magnetization of hard superconductors," *Phys. Rev. Lett.*, vol. 8, no. 6, pp. 250–253, Mar. 1962.

[36] S. Awaji, K. Kajikawa, K. Watanabe, H. Oguro, T. Mitose, S. Fujita, M. Daibo, Y. Iijima, H. Miyazaki, M. Takahashi, and S. Ioka, "AC losses of an HTS insert in a 25-T cryogen-free superconducting magnet," *IEEE Trans. Appl. Supercond.*, vol. 25, no. 3, pp. 1–5, Jun. 2015.

[37] F. Gu, Y. Zhao, L. Zhong, X. Duan, M. Song, B. Zhang, Z. Li, and Z. Hong, "Numerical study on magnetization losses in soldered-stacked-square (3S) HTS wires with 1 mm width," *IEEE Trans. Appl. Supercond.*, vol. 29, no. 2, pp. 1–5, Mar. 2019.
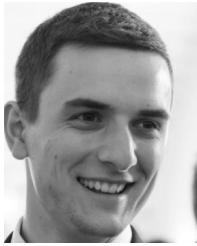
ANDREA ZAPPATORE received the M.Sc. degree in energy and nuclear engineering and the Ph.D. degree in energetics from Politecnico di Torino (PoliTo), Turin, Italy, in 2016 and 2021, respectively. He is currently an Assistant Professor with PoliTo. He received the EUROfusion Researcher Grant for the development and validation of quench and AC loss models for high temperature superconducting cable-in-conduit conductors for the EU-DEMO central solenoid. He has coauthored 35 articles published in international journals, focused on computational modeling in nuclear fusion systems and components. His research interests include the development, verification, validation, and application of new modeling tools for both low and high temperature superconducting magnets, and the computational fluid dynamics modeling of high heat flux components and accidental scenarios.

DAVIDE UGLIETTI received the Ph.D. degree in physics from the University of Geneva, Geneva, Switzerland, in 2006. He was with Pirelli Cables and Systems, Milan, working on AC losses in Bi2223 power transmission cables, from 1998 to 2000. working on microstructure and electromechanical characterization of Nb3Sn wires. From 2007 to 2010, he was with the National Institute of Material Science, Tsukuba, Japan, where he has engaged on the development of coated conductor high field insert coils. Since 2010, he has been a Scientist with the Swiss Plasma Center, École Polytechnique Fédérale de Lausanne, Villigen, Switzerland, working on HTS for high field inserts and for large fusion magnets.

• • •

GIANLUCA DE MARZI received the M.Sc. degree (cum laude) in physics and the Ph.D. degree in material sciences from the University of Rome La Sapienza, Italy, in 1996 and 2000, respectively. He is currently a Staff Researcher with the Superconductivity Laboratory, Italian National Agency for New Technologies, Energy and Sustainable Economic Development (ENEA), Frascati, Rome. His current research activities are focused on the design and manufacturing of superconducting cables, conductors, and magnets, for nuclear fusion experiments. He has a task responsible for the design of the superconducting magnet system's current feeders for the Divertor Tokamak Test (DTT) facility. He is a Technical Editor of the IEEE TRANSACTIONS ON APPLIED SUPERCONDUCTIVITY.